CHAPTER-4

Conduction through Carbon Atomic Chain attached to Armchair and Zigzag Edged Graphene Electrodes

At the present state of human knowledge quantum mechanics can be regarded as the fundamental theory of atomic phenomena.

-L. I. Schif

Ballistic transport through carbon atomic chain (CAC) attached to relaxed armchair graphene (ACG), zigzag graphene (ZZG) and unrelaxed armchair graphene (UACG) electrodes have been investigated, as a function of energy measured from Fermi level. Our computed results show that the equilibrium conductance of CAC attached to ZZG-electrodes tends to zero over a wide energy range across Fermi level. Similar behaviour of conductance is not seen when ZZG electrodes are replaced by ACG electrodes. CAC connected to ACG electrode is found better conducting as compared to CAC connected to ZZG electrode. The computed conductance, for a fixed energy value, strongly depends on whether CAC is attached to ZZG, ACG or UACG electrodes, suggesting that transport through electrode-CAC-electrode system depends on electrode edge structure. On comparing conductance of CAC connecting to graphene electrodes with that of CAC attached to metallic (Al) electrodes, we find that replacement of metallic electrode by graphene makes conductance smoother over wider energy range.

4.1. Introduction

Organic molecules are characterized by an amazingly wide variety of structures and the properties that originate from the combination of *sp*, sp^2 and sp^3 hybridisations of carbon atoms. There have been tremendous theoretical as well as experimental efforts to understand the synthesis and electronic characteristics of carbon atomic chains (CAC) with *sp*-bonding and graphene with sp^2-bonding because of their novel characteristics and possibility of their use in pure carbon based nano circuitry. It has been predicted that co-existence of *sp* and sp^2 bonding in a system gives rise to very interesting optical and electronic properties [1, 2]. Recently, two experimental groups [3, 4] have independently realized stable and rigid carbon atomic chains by employing energetic electron irradiation on graphene sheet inside a transmission electron microscope (TEM). These chains exhibited remarkably good stability with a length up to few nanometres even under the irradiation of 120 keV electron beams. The possibility of stabilizing *sp* chains in cluster assembled nanostructured carbon films [5] and inside carbon nanotubes [6, 7] has also been demonstrated suggesting that pure carbon sp^2 systems containing *sp* hybridisation can be synthesized. Recent experiments [8] suggest that cumulenic oligomers can be stabilized in a sp^2 carbon matrix and can be used to control the electrical properties and the nanostructure of the material by controlling the density and the decay of *sp* metallic chains [9]. It has also been predicted that there is possibility to control the nanowire conductance [10], optical properties, and spin magnetization, purely by twisting its sp^2 termination and modifying the electronic states near the Fermi energy (E_f), using torsional strain. The *sp*-sp^2 hybridisation present in these edge structures results in delocalized states across the whole molecule and opens a channel for transport. Due to its exotic electronic properties electron transport in CAC attached to metallic electrodes has been subject of wide interest during last decade [11-14]. However, it is very difficult to synthesize experimentally CAC-metal junctions and it would be even more difficult to make them

reproducible as manipulation of parameters related to surface morphology, contact site, orientation, bond angle is not possible at least as on today. This may lead to remarkable difference of few orders of magnitude in theoretical prediction and experimental values of conductance. On the other hand, experimental realization of CAC connected to graphene is very promising from view point of its possible application as basic unit in more complicated future electronic-circuits. Electron transport through CAC attached to zigzag graphene has recently been described by analytical model with the use of noninteracting electron approximations [15] and it was predicted that the electron transports via narrow resonant states in the chain, which arise due to strong reflection at the junctions. Width and the position of the resonance states depend on the length of the chain and its coupling to the leads. However, there exist no comparative investigations on electronic transport through CAC attached to armchair and zigzag graphene electrodes. The main objective of this paper has been to study the edge effects of graphene electrodes on electron transport through the CAC. Therefore, we have not considered spin-polarization effects on transport properties of CAC attached to zigzag and armchair graphene nanoribbons, as has been reported recently [16, 17].

The exciting electronic and transport properties of both CAC and graphene, possibility of the use of CAC connected to graphene leads as basic unit for more complicated futuristic electronic-circuits and the theoretical predictions that have been followed by experimental realization motivated us to investigate computationally the electronic transport through CAC connected to armchair graphene (ACG) and zigzag graphene (ZZG) electrodes. This is in continuation of our earlier theoretical investigations on transport through atomic chains of C-Si [18] and of C-H-S [19] which were attached to Al-electrodes.

4.2. Computational Details

Graphene has been believed to support ballistic transport even at room temperature [20]. The nanometric dimension of CAC is well below the electron mean free path and therefore, the resistive processes of diffusive and of inelastic origin are negligible and the electron transport is essentially ballistic even at room temperature [21]. At molecular level, adsorption-induced modification of molecular states is larger than the field-induced effect for low bias regime. Further, there are many complications in fabricating stable atomic chains that are capable of sustaining high bias voltages. Therefore, accurate modelling of the electronic processes at equilibrium is critical for determining low bias transport characteristics. In view of this, we have investigated ballistic conductance properties in a linear regime with zero applied bias and neglected the field-induced effects. The exchange-correlation energy is evaluated within Perdew and Zunger formula for local density approximation (LDA), which provides good results in case of organic molecules, noble metals and alkali metals. However, LDA does not incorporate spin-polarization effects, which could play an important role in magnetic description of problem of conduction through CAC attached to graphene electrodes. Valence electrons are explicitly considered using norm conserving pseudopotentials to account for core-valence interactions [22] with a wave function cut off of 60 Ry or charge cut off of 240 Ry. The Monkhorst-Pack sampling of (2,10,10) has been employed. To obtain electron transmission at energy, the generalized Bloch states, consisting of propagating and evanescent states, are constructed first, which are solution of the Kohn-Sham equation at that energy of hypothetical infinite lattice-periodic leads. These states are then used to construct the scattering states of the entire lead-nanocontact-lead system and to calculate the transmission function [21].

The geometries studied by us consist of a finite central resistive region (CRR) connecting to two semi-infinite electrodes. The CRRs, as shown in Figs. 4.1a, 4.2a and 4.3a are consisting

of CAC sandwiched between several buffer lead layers. The number of lead layers is chosen so that potential at the interface between central resistive region and left as well as right electrodes are bulk-like. The Hamiltonian matrices for semi-infinite left and right electrodes are obtained from standard first-principles calculations on bulk periodic systems. For ZZG and ACG calculations we first relaxed the electrode supercell for minimising inter-atomic forces to values smaller than 0.0025eV/Å. We then relaxed the CRR consisting of 9 atom long CAC and 2-3 hexagonal rings long layers of left and right electrodes in *z*-direction as is shown in Figs. 4.1a, 4.2a and 4.3a. The electrode supercell sizes in y and z directions are chosen in such a way that there is no vacuum layer introduced between two consecutive periodic images. Moreover, a supercell size in y direction is large enough (~ 13 Å) to prevent the interaction between periodic images of atomic chains. The distance between two graphene layers in *x*-direction is kept 10 Å in case of ZZG – CAC- ZZG while 13 Å in case of ZZG – CAC - ZZG, UACG – CAC- UACG and ACG – CAC- ACG structures to avoid any interaction between layers. In CRR, we relaxed only two rows of atoms of left and right graphene leads which are closest to CAC. Positions of atoms in other rings are kept fixed to bulk values obtained from relaxation of electrode supercell. Therefore, the potential at the end surface of extended molecule match well with electrode potential.

On structural relaxation of CAC attached to ACG leads, CAC get bonded to ACG via sp^3 bond and forms a pentagon at the contact, leading to subsequent changes even in the positions of atoms which are away from the contact. The pentagon formed at the CAC-ACG contact has also been observed experimentally [3, 4]. For such cases, we added one extra layer of hexagonal rings in *z*-direction for matching the surface atom potential of CRR with electrode surface potential. The structure relaxation of CAC attached to ACG electrode modifies the geometry remarkably. Therefore, to know exactly the effects introduced by edge structures of graphene electrodes, we also computed transport properties of CAC attached to unrelaxed

armchair graphene (UACG) electrodes. To compare the conductance of graphene-CAC-graphene system with that of an ideal contact, we also computed conductance for ACG attached to ACG electrodes (i.e. ACG-ACG-ACG system) and ZZG attached to ZZG electrodes (i.e. ZZG-ZZG-ZZG system).

4.3. Results and discussion

Our computed results show that the average C-C bond length in CAC (*sp*-hybridisation) is smaller than that in the graphene edge structure (mainly sp^2-hybridisation). The shorter bond length results in more valence electrons distribution around bonds and corroborates the bond strength. Atoms in CAC are more stable in comparison with edge atoms of the graphene electrode. It can therefore be inferred that there is higher probability of breaking of chain from its contact with graphene edge as compared to breaking from middle of the chain. The bond lengths between different C-atoms of CAC have minor bond length alternation and lay in the ranges of; (i) 1.28 Å to 1.30 Å for ACG, (ii)1.25 Å to 1.28 Å for ZZG, and (iii) 1.28 Å to 1.32 Å for UACG, as can be noted from Figs. 4.1a, 4.2a and 4.3a, respectively. The minor changes in bond lengths can be due to contact of end atoms of CAC with graphene edge. Our computed bond lengths closely match with empirical bond length (=1.34 Å) for double bond between carbon atoms. It can therefore be concluded that our computationally synthesized CAC is of cumulene-type. In agreement with previously reported results, our findings suggest that sp^2-kind termination produces highly stable cumulene-type structures that are characterized by a bond length alternation [23]. Calculations on infinite carbon chains indicate that polyynes are energetically more stable than cumulenes due to Peierls distortion [24]. However, for finite length cumulene chains, the enhancement in energy is not significant even at 0 K temperature [13]. The bond lengths between C-atoms in CAC and in

ZZG-electrodes have been found closely matching with previously reported results [3, 16, 17].

The computed values of transmission co-efficient (T) for CAC attached to ZZG, UACG and ACG electrodes are plotted in Figs. 4.1b, 4.2b and 4.3b, respectively as a function of energy ε measured from Fermi energy E_f that is set equal to zero. We computed T for per spin channel, as our electrode-chain-electrode system considered in this paper is non-magnetic. The total transmission co-efficient can be obtained simply by doubling our reported values of T. As our main objective has been to study the edge effects of electrodes on transport through CAC, we have not considered magnetic description of problem and hence used LDA instead of LSDA. Further, for a 9 atom CAC attached to armchair or zigzag edged graphene electrode, majority and minority spin transmission curves do not differ significantly from each other [16].

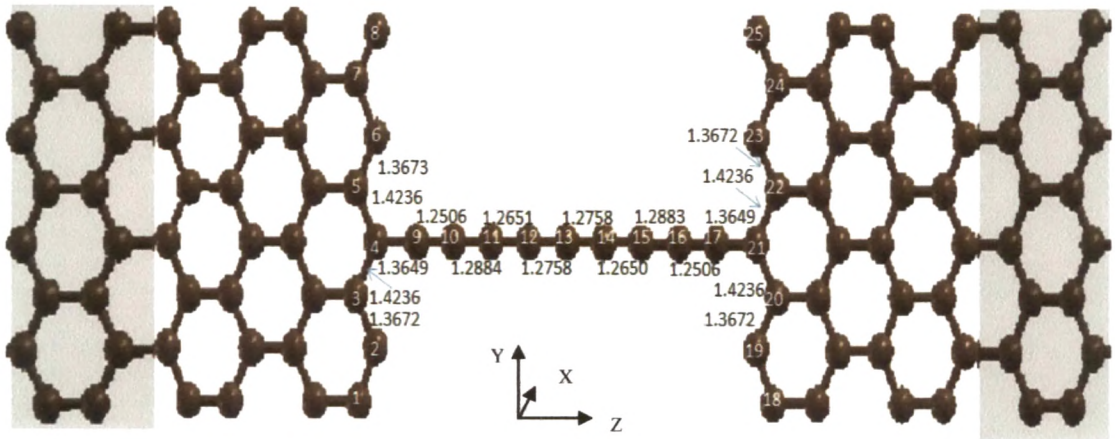

Figure 4.1a: The relaxed final geometry comprising of carbon atomic chain CAC connected to semi-infinite ZZG leads on both left and right sides. The electrode supercell is marked as the shaded area.

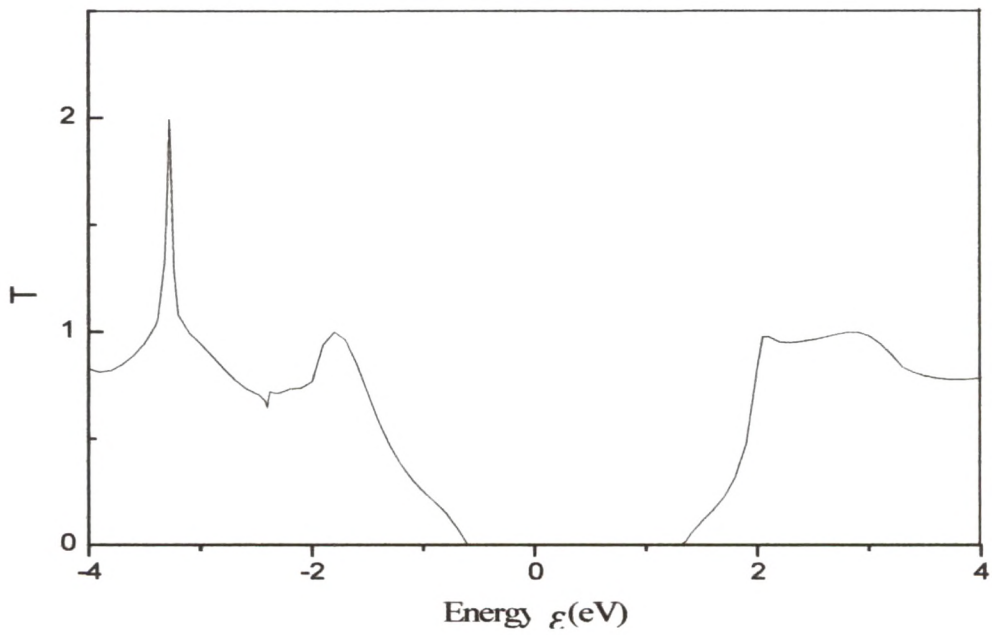

Figure 4.1b: The computed T as a function of ε (measured from E_f=0), for the ZZG - CAC - ZZG system.

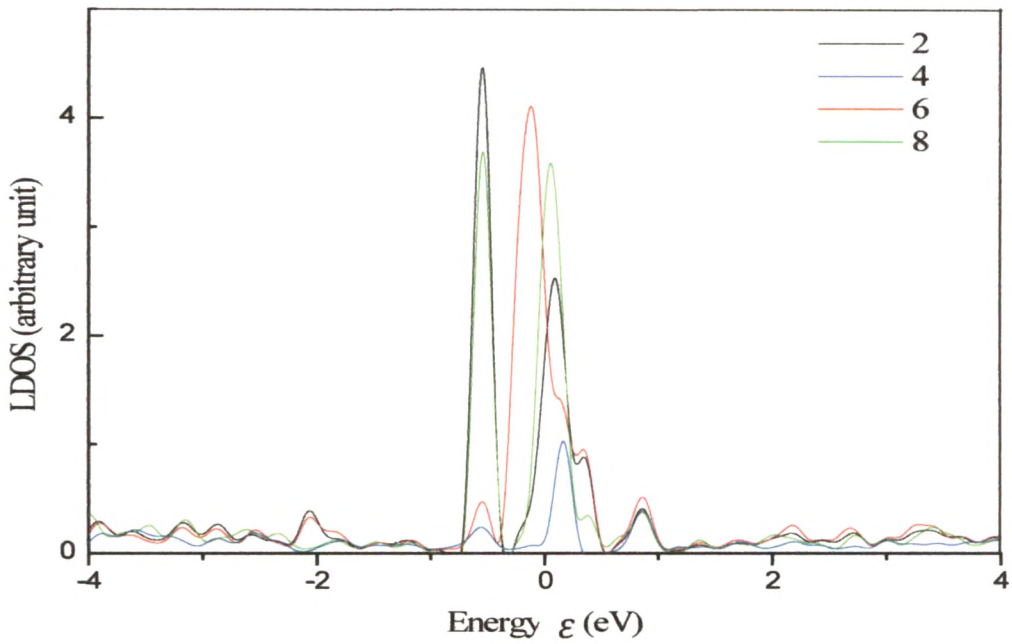

Figure 4.1c: The local density of states (LDOS) contributed by *P* orbitals of atoms marked as 2, 4, 6, 8, 9 in Fig. 1a for CAC connected to ZZG, are plotted as a function of ε.

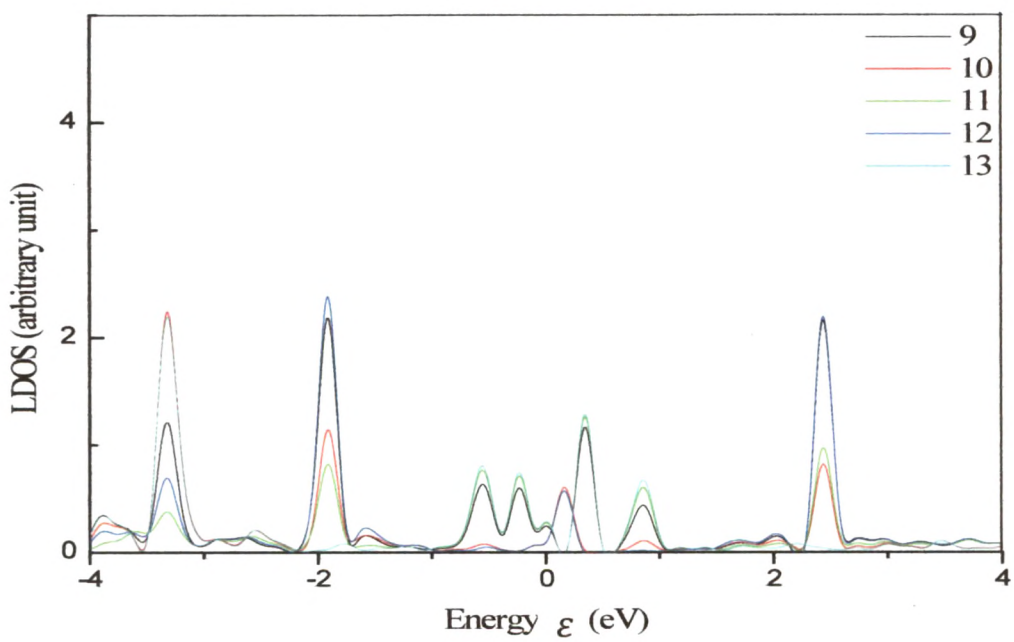

Figure 4.1d: Same as Fig. 1c for atoms marked as 9, 10, 11, 12, 13.

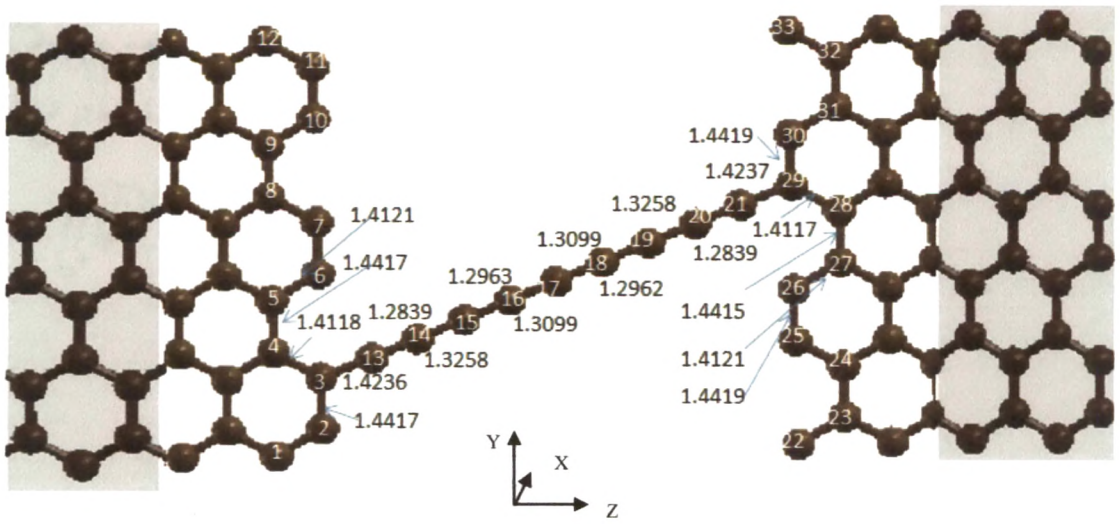

Figure 4.2a: The relaxed final geometry comprising CAC connected to semi-infinite unrelaxed armchair graphene (UACG) leads on both left and right sides. The electrode supercell is marked as the shaded area.

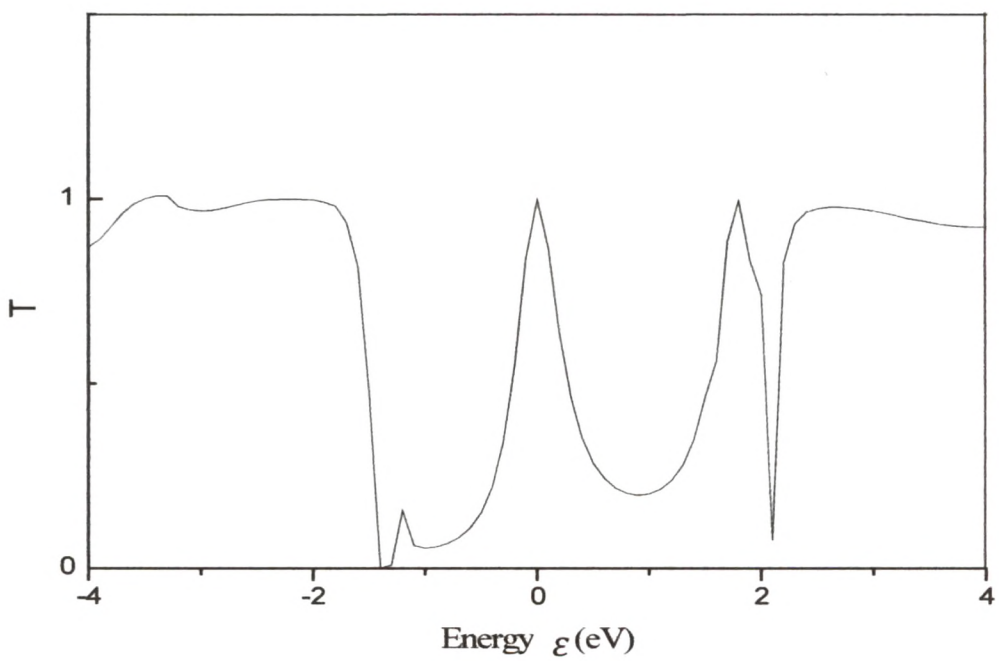

Figure 4.2b: The computed T as a function of ε (measured from E_f =0), for the UACG – CAC- UACG system.

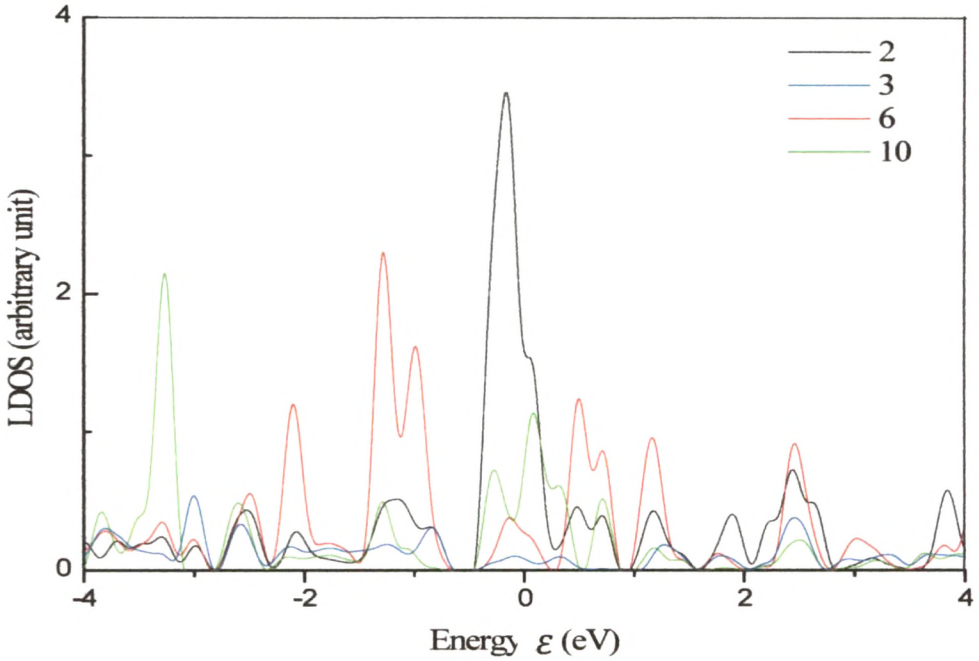

Figure 4.2c: The local density of states (LDOS) contributed by *P* orbitals of atoms marked as 2, 3, 6, 10 in Fig.2a for CAC connected to UACG, are plotted as a function of ε.

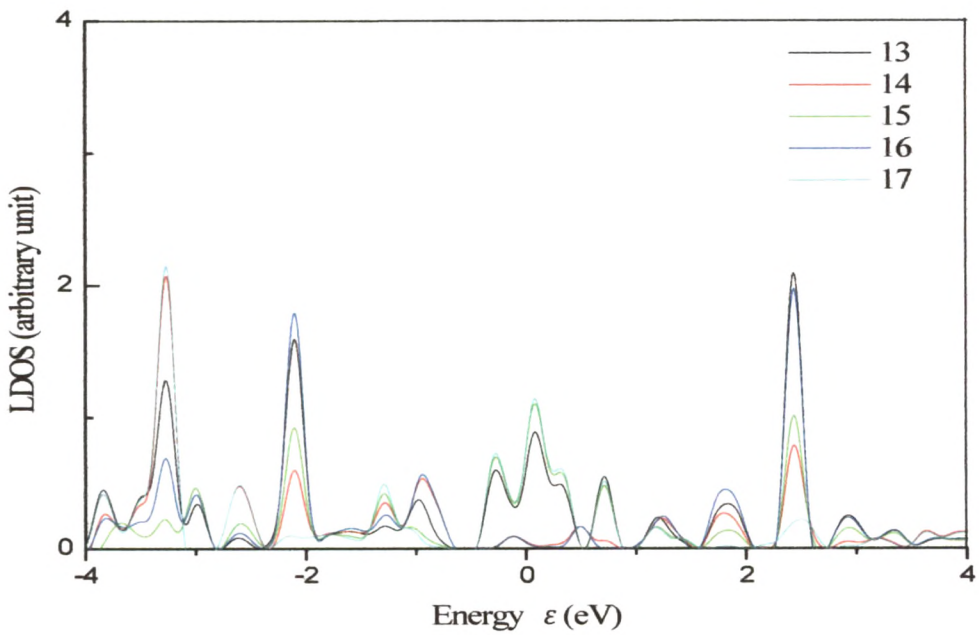

Figure 4.2d: Same as Fig. 2c for atoms marked as 13, 14, 15, 16, 17.

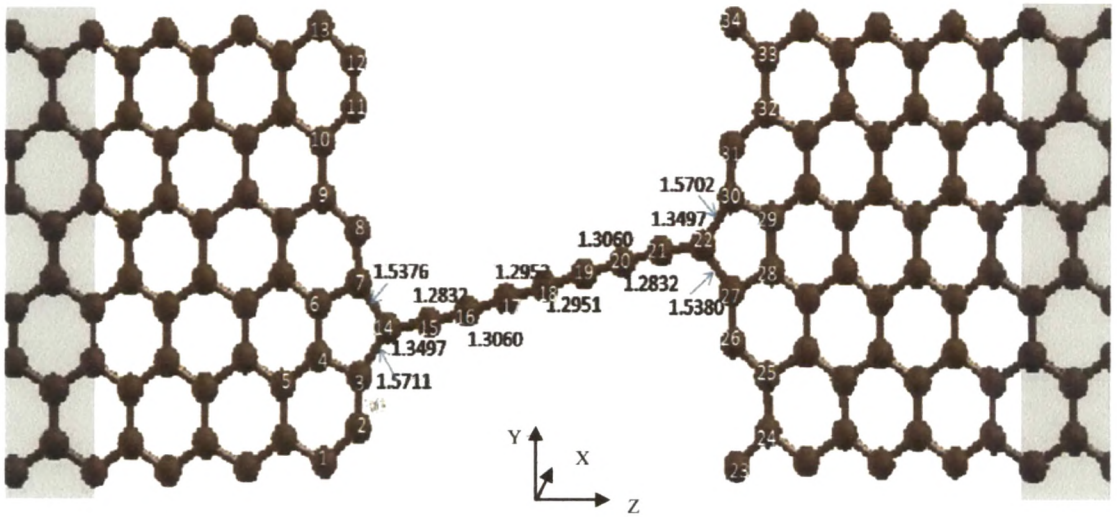

Figure 4.3a: The relaxed final geometry comprising CAC connected to semi-infinite armchair graphene (ACG) leads on both left and right sides. The electrode supercell is marked as the shaded area.

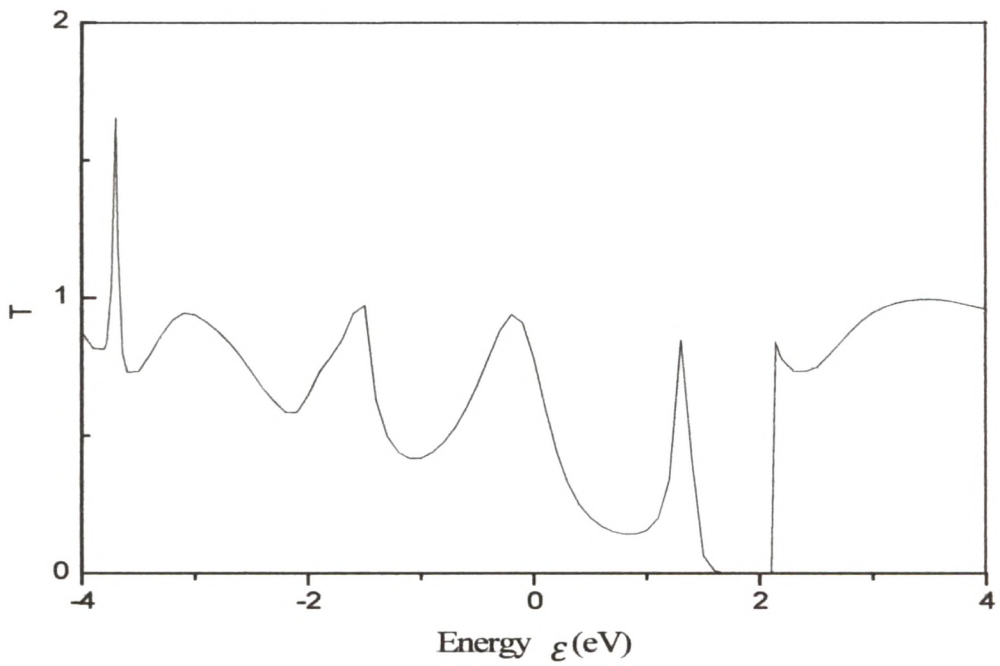

Figure 4.3b: The computed T as a function of ε (measured from E_f=0), for the ACG – CAC-ACG system.

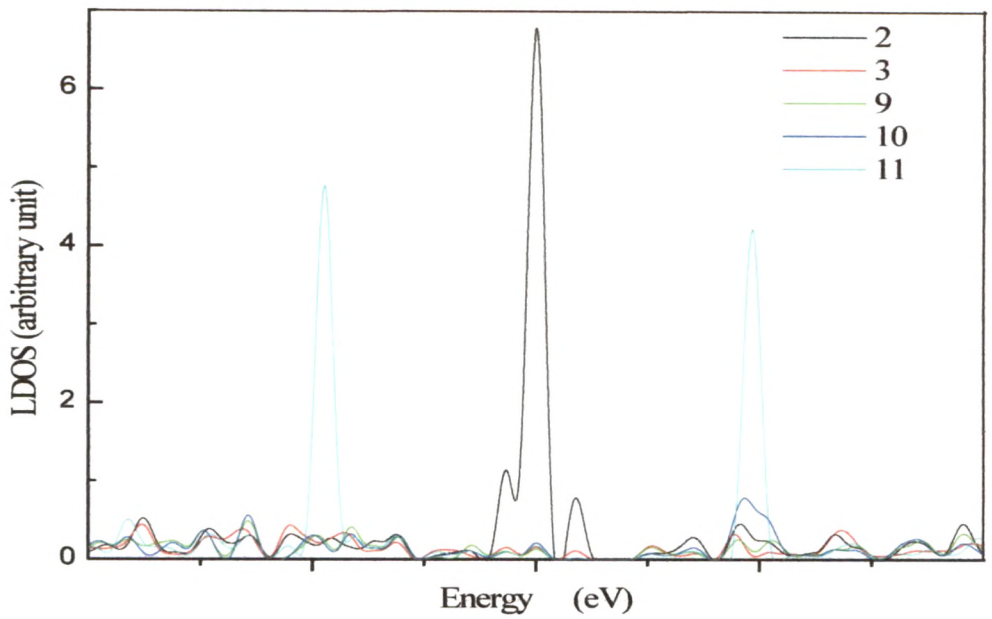

Figure 4.3c: The local density of states (LDOS) contributed by *P* orbitals of atoms marked as 2, 3, 9, 10, 11 in Fig.3a for CAC connected to ACG, are plotted as a function of ε.

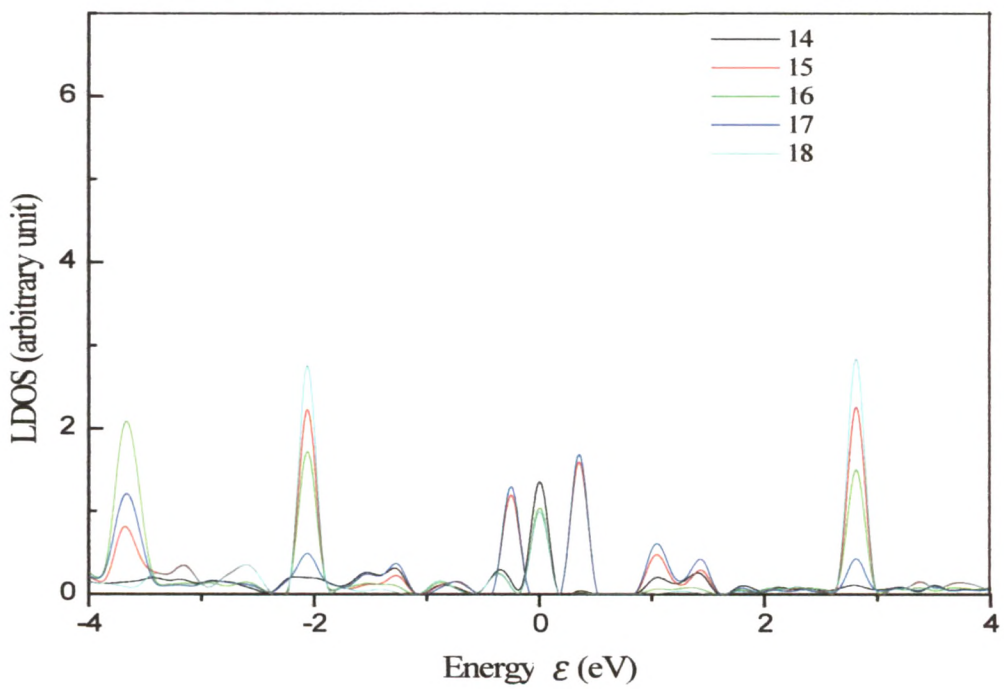

Figure 4.3d: Same as Fig. 3c for atoms marked as 14, 15, 16, 17, 18.

In all three cases of CAC attaching to ZZG, UACG and ACG electrodes, computed T values are found close to 1 for $\varepsilon \geq 2$ eV and $\varepsilon \leq -2$ eV, with continuous T-curve covering a broader energy range showing nearly perfect energy level matching. As can be seen from Fig. 4.1b, T-curve for CAC attached to ZZG electrode shows zero transmission for a considerably larger energy range of; $-0.75\ eV \leq \varepsilon \leq 1$. For rest of the energy range, the chain is highly conducting as it displayed a larger plateau in T of significant height. Contrary to this, in cases of CAC attached to ACG and UACG electrodes, there is no energy region for which computed T goes to zero, as is depicted in Figs. 4.2b and 4.3b. In case of CAC attached to UACG electrode, T exhibits peaks in energy regime around E_f. Our computed value of equilibrium conductance at Fermi energy, G(E_f) for UACG, ACG and ZZG are; $0.9998G_0$, $0.77899G_0$ and zero, respectively. In the cases of ACG and UACG electrodes, our computed T is nonzero for most of the energy range. However, there are two deeps at around $\varepsilon = 2$ eV and $\varepsilon = -2$ eV for the case of UACG-electrode and there is one deep at $\varepsilon = 2$ eV in ACG-electrode case.

A larger peak value (≈ 2) in T curve has been observed near $\varepsilon = -3$ eV for ZZG case, as is seen in Fig. 4.1b. The similar peak has also been observed in T-curve displayed in Fig. 4.3b, for the case of CAC attached to ACG forming pentagon at the contact. To testify the existence of peak more rigorously and to make sure that it is not a manifestation of mathematical irregularity, we computed T in this energy region using energy interval of 0.04 eV unlike the case for other energy regions where T has been computed with the use of energy interval of 0.1 eV. We found that the peak in T does really exist at around $\varepsilon = -3$ eV. The peak can be attributed to the fact that the CAC is attached to C-atom numbered 4 of ZZG-electrode in which atom-4 is connected to atom numbered 3 and 5, which are sp^2 hybridised, as is exhibited in Fig. 4.1a. A similar peak has been seen in Fig. 4.3b plotted for CAC attached to ACG-electrode forming pentagon at the contact atom numbered 4 which is

connected to sp^2 hybridized atoms 3 and 7 of electrode. In case of CAC attaching to atom numbered 3 of UACG-electrode, which connects to C-atom numbered 2 and 4 having *sp* and sp^2 hybridisations, respectively.

Figs. 4.1c, 4.2c, 4.3c depict LDOS contribution of electrode edge atoms for ZZG, UACG and ACG electrodes, respectively. The LDOS contribution from chain atoms when CAC attached to ZZG, UACG and ACG electrodes are plotted in Figs. 4.1d, 4.2d and 4.3d, respectively. It is strikingly evident from the figures that contribution to LDOS from CAC atoms is much smaller than that from electrode edge atoms. The LDOS-curves for CAC attaching to ZZG-electrodes are plotted in Figs. 4.1c and 4.1d. The atoms of graphene edge, which are numbered as 2, 6, 8, 19, 23 and 25 and have sp-hybridisation, are contributing larger peaks with maximum contribution coming from P_z orbitals, while the CAC atoms numbered as 9 to 17 with sp hybridisation give rise to the peaks contributed by P_y orbitals. All other atoms (numbered 1, 3, 5, 7), in electrode edge having sp^2 hybridisation, exhibit nearly zero LDOS (not shown in figures) with very little contribution from P_x orbitals in the energy range away from E_f. Similar trend has been observed for the cases of CAC attached to ACG as well as UACG-electrodes. The basic difference between LDOS of relaxed and unrelaxed armchair graphene electrodes is seen in the form of change in height of peaks. Peaks with smaller heights convert to larger height and vice versa on changing ACG-electrode with UACG.

As is seen from Fig. 4.3a for CAC attaching to ACG electrodes, atoms numbered as 2, 8, 26, 31 are in identical positions and surroundings and they all display identical LDOS-curves, from which LDOS curve of atom-2 is depicted in Fig. 4.3c, having peak at E_f, contributed maximally by P_z orbital. The graphene electrodes are periodic in *y*-direction and hence atoms numbered 23 and 34 are symmetric to atoms numbered 11 and 12. These atoms are edge

atoms of the ring which is situated one hexagonal ring away from the pentagon formed at the contact of CAC and ACG-electrode. The atoms numbered 11, 12, 23 and 34 give rise to identical LDOS-curves having maximum contribution from P_z orbital. However, there are two peaks in LDOS appearing at ε = 2 eV and ε = -2 eV. The PDOS curves (not shown in figures) of all CAC-atoms, except terminal atoms, are mainly contributed by P_y orbital and almost zero contribution comes from P_z orbital. PDOS and its peak at E_f for terminal atoms 14 and 22 of CAC are contributed mainly from P_x orbital and a very little contribution comes from other orbitals. From LDOS curves of all atoms in a system of CAC connecting to ACG-electrode, we can infer that the atoms having *sp* hybridisation exhibit large peaks, while atoms having sp^2 hybridisation display negligibly small peaks. Atoms at edge structure of ACG-electrode that have *sp* hybridisation get major contribution to PDOS from P_z orbitals, while atoms of CAC with *sp* hybridisation have major contribution to PDOS from P_y orbitals.

On comparing the present results of CAC connecting to graphene electrode sheet with that of CAC attached to Al-electrode, which were reported by us in past [17], we find that the use of graphene electrode in place of Al-electrode makes conductance highly smooth, almost constant over a wider energy range. We conclude that the wiggles in T curve as a function of energy for CAC attached to Al-electrode might be manifestation of irregularity in matching of energy levels of electrode and CAC. As a remedy to this, a Sulphur atom has been suggested to be placed at molecule-electrode junction, which has a better chemical absorption. However, it is very difficult experimentally to bring such an extra atom to specific site.

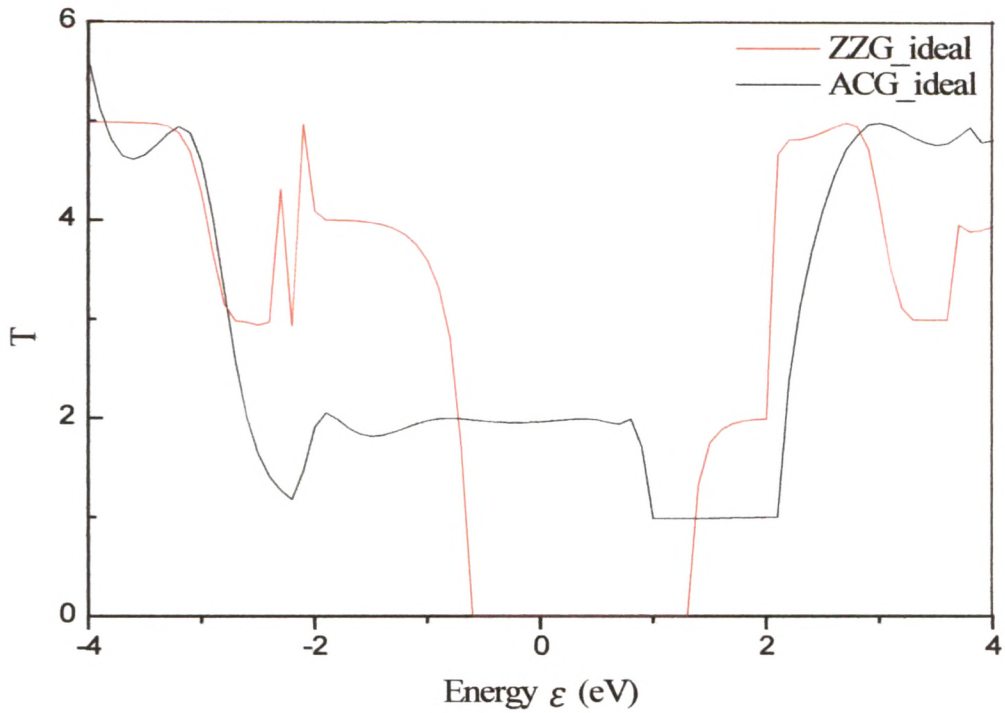

Figure 4.4: The computed T as a function of ε (measured from E_f =0), for the ZZG-ZZG-ZZG and ACG-ACG-ACG systems.

The conductance curves for ideal contact systems comprising of ACG attached to ACG electrodes and ZZG attached to ZZG electrodes are plotted in Fig. 4.4. The ACG-ACG-ACG system shows nonzero conductance over entire investigated energy range. Contrary to this, T for ZZG-ZZG-ZZG system approaches to zero for a broader energy range covering E_f. T for ZZG-CAC-ZZG system also exhibit similar behaviour as is seen from Fig. 4.1b. We thus can conclude that, the zero transmission regions observed in case of CAC attaching to ZZG are manifestation of ZZG electrodes.

4.4. Conclusions

Motivated by recent experimental realization of graphene structures bridged by CAC, we have optimized the graphene-CAC-graphene system and computed their ballistic conductance. In our structures, armchair and zigzag edged graphene acted as the electrode. The CAC connecting to graphene sheet makes a stable geometry, in which end atoms of the chain form sp^2 hybridisation, whereas hybridisation of chain atoms is sp-type. It is found that the difference in graphene edge geometry significantly alters the transport behaviour of system. The system of CAC connected to ZZG gives rise to zero T values over a wider energy range across Fermi level E_f. The transport properties are remarkably altered on replacing ZZG electrodes by ACG or UACG electrodes, suggesting that the transport depends on electrode edge structure geometry. Replacement of metallic electrode by a graphene electrode provides a more stable junction and better transport properties.

4.5 References

[1] R. H. Baughman, H. Eckhardt, and M. Kertesz, J. Chem. Phys. **87** (1987) 6687-6699.

[2] N. Narita, S. Nagai, S. Suzuki and K. Nakao, Phys. Rev. B **58** (1998) 11009-11014.

[3] C. Jin, H. Lan, L. Peng, K. Suenaga, S. Iijima, Phys. Rev. Lett. **102** (2009) 205501.

[4] A. Chuvilin, J. C. Meyer, G. Algara-Siller, Ute Kaiser, New Journal of Physics **11** (2009) 083019.

[5] L. Ravagnan, F. Siviero, C. Lenardi, P. Piseri, E. Barborini, P. Milani, C. S. Casari, A. Li Bassi, and C. E. Bottani, Phys. Rev. Lett. **89** (2002) 285506.

[6] Zhenxia. Wang, Xuezhi Ke, Zhiyuan Zhu, Fengshou Zhang, Meiling Ruan, Jinqing Yang, Phys. Rev. B **61** (2000) R2472- R2474.

[7] X. Zhao, Yoshinori Ando, Yi Liu, Makoto Jinno and Tomoko Suzuki, Phys. Rev. Lett. **90** (2003) 187401.

[8] L. Ravagnan *et al.*, Phys. Rev. Lett. **98** (2007) 216103.

[9] S. Bhattacharya, S. J. Henley, E. Mendoza, L. Gomez-Rojas, J. Allam and S. R. P. Silva, Nat. Mater. **5** (2006) 19-22.

[10] K. H. Khoo, J. B. Neaton, Y. W. Son, M. L. Cohen, S. G. Louie, Nano Lett. **8** (2008) 2900-2906.

[11] N. D. Lang and Ph. Avouris, Phys. Rev. Lett. **81** (1998) 3515-3518.

[12] B. Larade, J. Taylor, H. Mehrez, and H. Guo, Phys. Rev. B **64** (2001) 075420.

[13] S. Tongay, R. T. Senger, S. Dag, and S. Ciraci, Phys. Rev. Lett. **93** (2004) 136404.

[14] Z. Crljen and G. Baranovic, Phys. Rev. Lett. **98** (2007) 116801.

[15] W. Chen, A. V. Andreev, G. F. Bertsch, Phys. Rev. B **80** (2009) 085410.

[16] Zeila Zanolli, Giovanni Onida and J.-C. Charlier, ACS Nano **4** (2010) 5174-5180.

[17] Joachim A. Furst, Mads Brandbyge and Antti-Pekka Jauho, arxiv:0909.1756v2 [cond-mat.mes-hall]

[18] S. K. Ambavale, A.C. Sharma, J. Comp. & Theo. Nanosci. **6** (2009) 1549–1555.

[19] S. K. Ambavale, A.C. Sharma, Physica E **42** (2010) 2026-2032.

[20] A. K. Geim, K. S. Novoselov, The rise of graphene, Nature Materials **6** (2007)183–191.

[21] A. Smogunov, A.D. Corso, E. Tosatti, Ballistic conductance of magnetic Co and Ni nanowires with ultrasoft pseudopotentials, Phys. Rev. B 73 (2006) 075418;

[22] We used pseudopotential C.pz-vbc.UPF for Carbon from the http://www.quantum-espresso.org distribution.

[23] L. Ravagnan, N. Manini, E. Cinquanta, G. Onida, D. Sangalli, C. Motta, M. Devetta, A. Bordoni, P. Piseri, P. Milani, Effect of Axial Torsion on sp Carbon Atomic Wires, Phys. Rev. Lett. **102** (2009) 245502.

[24] A. Abdurahman, A. Shukla, and M. Dolg, Ab initio many-body calculations on infinite carbon and boron-nitrogen chains, Phys. Rev. B **65** (2002) 115106.